Egyptian Journal of Aquatic Biology & Fisheries
Zoology Department, Faculty of Science,
Ain Shams University, Cairo, Egypt.
ISSN 1110 – 6131
Vol. 26(6): 887 – 908 (2022)
www.ejabf.journals.ekb.eg

Contribution of Seismic Attributes in Delineating the Hydrocarbon Reservoir of Abu Madi Formation, West EL Manzala Area, the Eastern Part of Onshore Nile Delta, Egypt

Salah Shebl[1], Mohamed Abu El-Hassan[2], Abeer A. Abuhagaza[1], Mousa Salama[1] , Ola Mohammed Eloney [1, *]

1 Exploration Department, Egyptian Petroleum Research Institute, Nasr City, Cairo, Egypt
2 Department of Geology, Faculty of Science, Monoufia University, Egypt
[*]**Corresponding Author: geo.ola.mohammed@gmail.com**

ARTICLE INFO

Article History:
Received: Nov. 20, 2022
Accepted: Dec. 21, 2022
Online: Dec. 29, 2022

Keywords:
Abu Madi Formation,
Velocity,
Time maps,
Attributes

ABSTRACT

In the Nile Delta province, approximately 88 trillion cubic feet (TCF) of gas reservoirs have been discovered. The main gas-producing rocks in EL Manzala Field are the Abu Madi Formation, a unit of gas-fertile rocks in the Nile Delta basin in the eastern part of the onshore Nile Delta, Egypt. Seismic data are the outputs of a convolution operation between the earth reflectivity and a source wavelet. Based on the results of the rock type analysis, the productive layers at the top and lower zones of Abu Madi Formation West El Manzala Field can be categorized into three units: good, moderate and low. In order to support the geologic interpretations for the area under study, the interpreter can gain more knowledge from conventional seismic data by using seismic characteristics. The seismic interpretation of Abu Madi Formation tops, average, interval velocity gradient maps, and time structure contour maps, followed by discussing the main attributes such as the envelope, RMS amplitude, instantaneous phase, instantaneous frequency, and relative acoustic impedance (RAI) are the most effective seismic features for displaying Abu Madi channel on the seismic sections. In addition, the study explained the existence of the sand reservoirs and the presence of hydrocarbon with different percentages in the Miocene section of the Manzalla gas field.

INTRODUCTION

After the recent gas discoveries onshore (e.g., Noras) and offshore (e.g., Zohr), the Nile Delta have become one of the biggest gas-producing provinces in Africa **(Shehata, 2008; Leila & Moscariello, 2019; Leila *et al*., 2020)**. The Nile Delta's main reservoir sources range in age from the Oligocene to the Late Pliocene. The potential for probable hydrocarbon accumulations in the Nile Delta was increased by the presence of various mature source rocks (Jurassic to Early Miocene), as well as structural and stratigraphic traps **(Abdel Aal *et al*., 1994; EGPC, 1994; Dolson *et al*., 2005)**. The Jurassic and upper Cretaceous-lower Paleogene source rock intervals were the main sources of the thermogenic gas, condensate, and light oil accumulations in the Nile Delta

(Vandre *et al.*, 2007; Leila & Moscariello 2017; El-Diasty *et al.*, 2020). The major hydrocarbon exploration targets, particularly in the onshore region, are different depositional facies (fluvial and estuarine) found in the Upper Messinian sequence of the Nile Delta (Abu Madi Formation) **(Dolson *et al.*, 2001; Salem *et al.*, 2005; Leila *et al.*, 2016, 2020)**. The quality of the Abu Madi reservoir facies is largely controlled by their initial depositional conditions, whereas the post-depositional attributes play a relatively minor role **(Salem *et al.*, 2005; Leila *et al.*, 2019)**. The studied area of West El Manzala Field occupies 82km² of the eastern part of the Onshore Nile Delta. It is located to the east of the Damietta Nile branch and on the western side of El Manzala Lake. Location and base map of the area under investigation are shown in Fig. (1), which is located between latitudes 31º 15', 31º 25' N and longitudes 31º 38', 31º 45' E. It is essential for effective reservoir management to have a comprehensive understanding of reservoir heterogeneity and rock type, but achieving this is hard due to the need for a variety of tools and methods for detection **(Mondal *et al.*, 2021)**. The present study tackled these issues via seismic interpretation using velocity gradient maps (average and interval), and time structure contour maps, as well as using seismic attributes to illustrate Abu Madi channel applying modern techniques of 2D seismic data reflection. The results of this study would improve the predictability of Abu Madi reservoir performance and guide the study area's developmental strategies.

Geologic Setting

The structural history of the Nile Delta is significantly influenced by the major tectonic features emerging throughout the Late Eocene and Early Miocene periods **(Said, 1990)**. The Red Sea, which was rifted from the Arabian plate is located near the northern edge of the NE-African plate, which ranges from the Cretan and Cyprus arc subduction zones to the Nile Delta. **Sestini (1995)** classified the Nile Delta into two provinces (Fig. 1): the Pliocene-Pleistocene sediments that were highly deposited in the Deep Offshore Nile Delta (more than 3500m in 4- 5 million years), which had a significant impact. It demonstrated post-Messianic faulting, particularly along the NNE and NE directions. While, the second province was that of the Nile Delta's onshore area, which was split into the North and South Nile Delta provinces by a hinge line (the flexure zone), representing a main structural sedimentary sub-province.

The existing tectonic structure has existed since the Oligocene due to the submergence of a once-emerging microcontinent in the region during the Paleocene and Eocene **(El-Gamal & El-Bosraty, 2008)**. The structure had a considerable unconformity at the shoulder of the Messinian section's main channel, making it a classic paleo-high. According to **Rizzini *et al*. (1978)**, there are three main geological cycles that make up the clastic deposits of the Nile Delta. The Miocene cycle, whose base is incompletely known, is mostly composed of shallow marine to non-marine sediments from the Sidi

Salem Fm, Qawasim Fm, and Abu Madi Fm as shown in Fig. (2). This major sea level fall caused the Mediterranean Sea's water level to drop significantly, which led to extensive erosion; the Mediterranean region was the place of the formation of enormous canyon incisions, and the development of the deposition core of the basin contains salt deposits **(Dolson *et al*., 2005)**. The re-connection with the open sea is assumed to have caused the transgression during the Pliocene period. From the Jurassic until the Early Cretaceous periods, rifting and extension occurred. This led to the construction of basins with an east-west trend, followed by widespread thermal sagging and subsidence with the development of shelf margins.

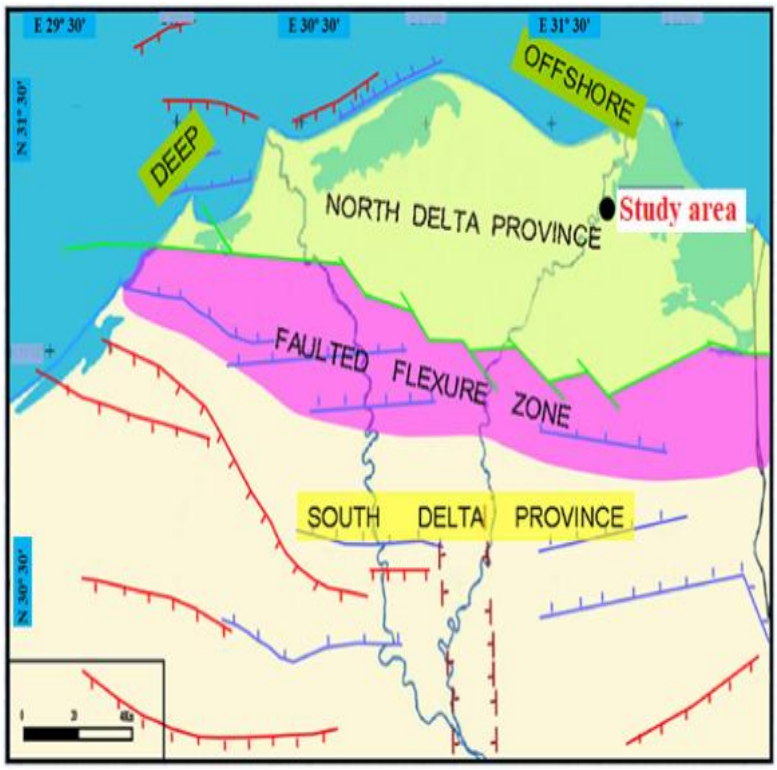

Fig. 1. The Main subsurface structures of the Nile Delta (Sestini 1989)

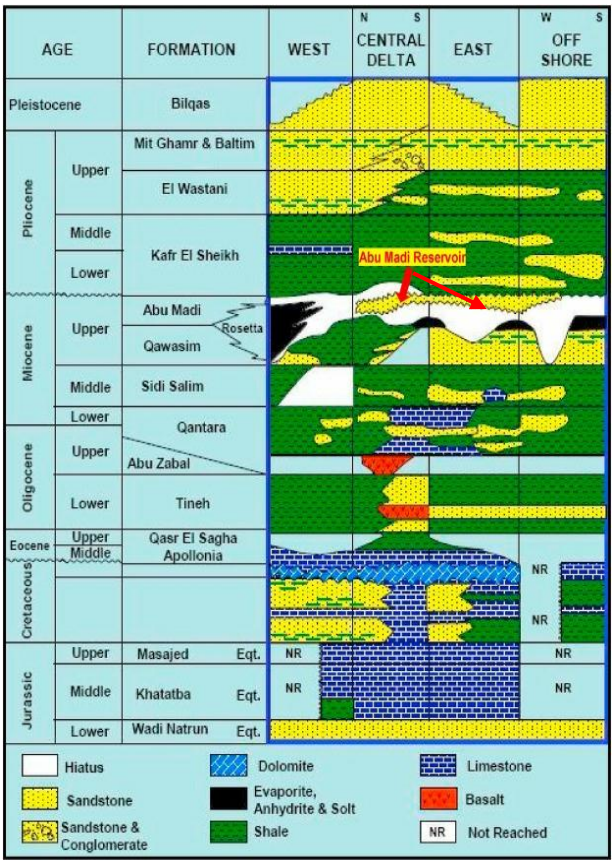

Fig. 2. Generalized Litho stratigraphic column of the Nile Delta, Egypt (EGPC, 1994)

MATERIALS AND METHODS

The present study was based on a complete subsurface data- set including both seismic lines and well logs from EL Manzala field. The dataset was analyzed and interpreted following a stepwise procedure in order to achieve the study objectives. Briefly, this study used the following methods: starting with constructing velocity maps (interval and average velocity maps) to show the distribution of both velocities that helps

revealing the variation of rock properties of the same formation, viz. varies in porosity, density and fluids.

In addition, the study used the piking of the different horizons of the interesting formation, plotting the faults and constructing the time structure contour maps to illustrate the structure affecting the target formations in study area.

Furthermore, the seismic enhancement attributes were used in the current work, including the signal envelope, instantaneous phase, instantaneous frequency, dominant frequency, relative acoustic impedance (RAI) and RMS amplitudes to assist our goals in detecting the difference in formation properties, especially that related to the presence of the hydrocarbon.

RESULTS AND DISCUSSION

4.1.Velocity analysis

The distance travelled in a unit of time is referred to as velocity. It has magnitude and direction because it is a vector quantity. Speed is the scalar quantity connected to velocity. In the oil and gas industry, three main forms of velocity are generally utilized. The first is called average velocity V_{avg}, which is calculated from the distance traveled per unit time, where the distance traveled is the total thickness of many layers or strata measured from the top of the uppermost layer to the base of the lowermost layer. The second is interval velocity V_{int}, representing the distance travelled per unit of time, where the distance travelled is equal to the thickness of a single, clearly defined layer or stratum. The third is called root-mean-square (rms) velocity V_{rms}, which is a statistical quantity calculated from V_{int} and Δt_{i} (two-way-time thickness of the layer).Velocity increases with the decrease of time. Interval velocity in the same layer of the same thickness and the same petrophysical propereties varies because of presence of different fluids with different porosity and density.

4.1.1 Average velocity gradient map on top of Abu Madi Formation

The center of this map (Fig. 3A), near to SF-3 and SF-6 wells, shows a rise on the upper Abu Madi's average velocity. In the north- west of F-1 and the south- east of SF-2, it declines. Minimum values are found on two sides of the map, in the south-east and north- west, where the value reaches 2226m/ s as seen in the maximum value of 2264m/ s existing from NE-SW. This indicates that, the velocity increases with dense rock of low porosity and dense fluid, while in the presence of high porous rock with low dense fluids such as gas, the velocity decreased.

4.1.2 Average velocity gradient map on top of Abu Madi Leve l

The average velocity gradient map drawn on top of Abu Madi level Ⅰ (Lower Abu Madi Ⅰ) (Fig. 3B) reveals velocity values that increase generally from the east to the

west. It contains two anomalies trend in the northeast- southwest direction. The maximum value attains about 2282m/ s lying to the west of SF-3 and SF-1 wells; meanwhile, the minimum value reaches about 2258m/ s and is located to the east of F-1 well. This can be explained as follows: on the presence of dense rock, low porosity and a dense fluid, the velocity increases; whereas, upon the existence of high porosity rock and low density fluids such as gas, the velocity decreases.

4.1.3 Average velocity gradient map on top of Abu Madi Level Ⅱ

The average velocity gradient map drawn on top of Abu Madi level Ⅱ (Lower Abu Madi Ⅱ) (Fig. 3C) delineating the velocity values increases regularly from the northeast to the southwest. The maximum value is about 2298m/ s in the west of SF-3 well, while the minimum value is 2264m/ s in the east of SF-1, SF-6 and the south of SF-2 well. This explains that, in the presence of dense rock with low porosity and dense fluid, the velocity increases, whereas it decreases in the presence of dense rock with large porosity and low density fluids such as gas.

4.1.4 Interval velocity gradient map on top of Abu Madi Formation

The interval velocity gradient map of Abu Madi Formation (Fig.4.A) illustrates the increase in the center reaching 2252m/ s near SF-6 and SF-3 wells; meanwhile, it decreases towards south- east in SF-2 well, and towards the northwest near F-1 well, where the minimum value reaches 2202m/ s. For the presence of various fluids present, each of which with a distinct porosity and density, the interval velocity in a layer with the same thickness and petrophysical characteristics might vary.

4.1.5 Interval velocity gradient map on top of Abu Madi Level Ⅰ

The interval velocity gradient map of top lower Abu Madi Ⅰ (Lower Abu Madi Ⅰ) (Fig. 4B) displays that, the velocity values increase generally in the southeast and the northwest and decrease in the center of the map, The maximum value attains about 4000 m/s lying to the west of F-1and SF-2 well, while the minimum values reaches 2600m/ s near SF-6 and SF-3 wells. The presence of various fluids with varying porosity and density causes variation in the interval velocity of a layer, with the same thickness and petrophysical characteristics.

4.1.6 Interval velocity gradient map on top of Abu Madi Level Ⅱ

The interval velocity gradient map on top Abu Madi level Ⅱ (Lower Abu Madi Ⅱ) (Fig. 4C) reflects that, the velocity values increase generally from the northeast to the southwest. The maximum value is about 3600m/ s in the southwest towards the west of SF-3 well and SF-6; meanwhile, the minimum value reaches about 2100m/ s, located to the southeast of SF-2 well. The presence of several fluids with varying porosity and density causes interval velocity to vary.

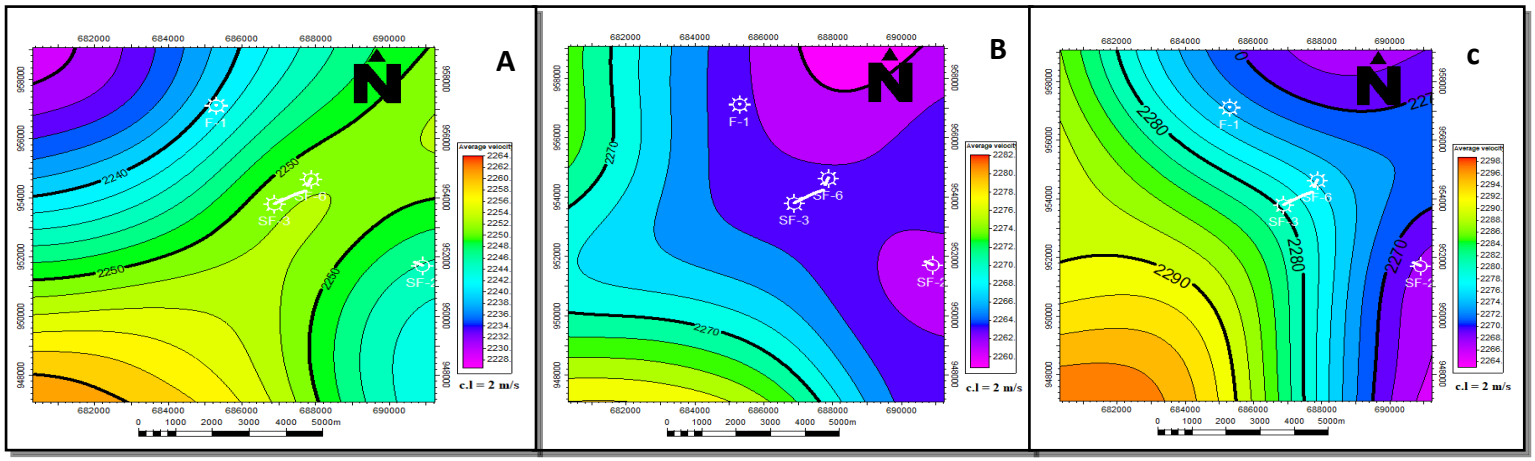

Fig.3. Average velocity gradient maps on top of (A) Abu Madi Formation; (B) Abu Madi Level Ⅰ, and(C) Abu Madi Level Ⅱ

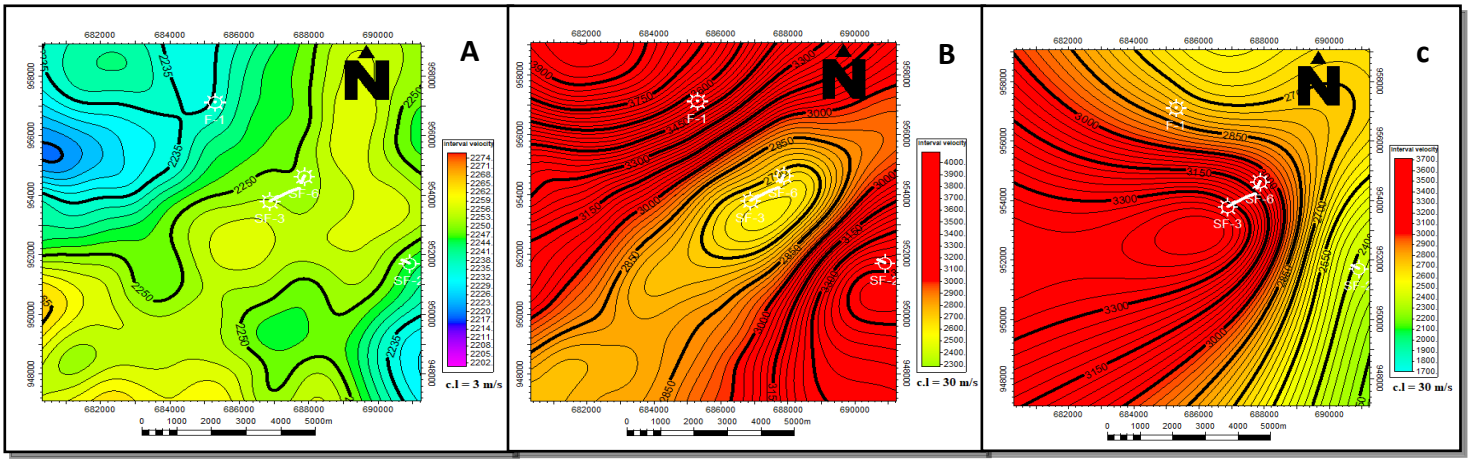

Fig.4. Interval velocity gradient maps on top of (A) Abu Madi Formation; (B) Abu Madi Level Ⅰ, and(C) Abu Madi Level Ⅱ

4.2 Seismic Interpretation

In processing seismic data, a step should be initially taken to increase its signal-to-noise ratio. Convolution of a source wavelet with the earth's reflectance produces seismic data. The available 2D reflection seismic profiles covering the study area are thoroughly analyzed as part of seismic interpretation (Fig. 5). This satisfies the criteria for a correct identification of the seismic series boundaries separating the Messinian Abu Madi succession. Moreover, by following the various reflection configurations and stratal terminations within Abu Madi succession, the internal seismic facies encountered were described **(Vail *et al.*, 1977; Pigott & Radivojevic 2010)**. The next work flow delinates the steps of seismic interpretation as shown in (Fig. 6).

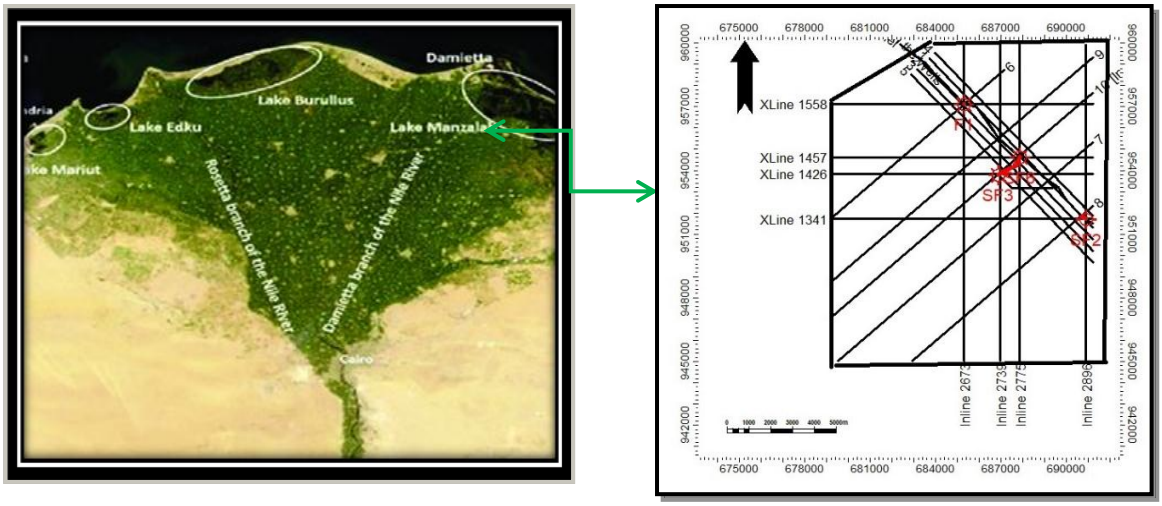

Fig. 5. Location of West El Manzala development lease, Onshore East Nile Delta and Wells in study area

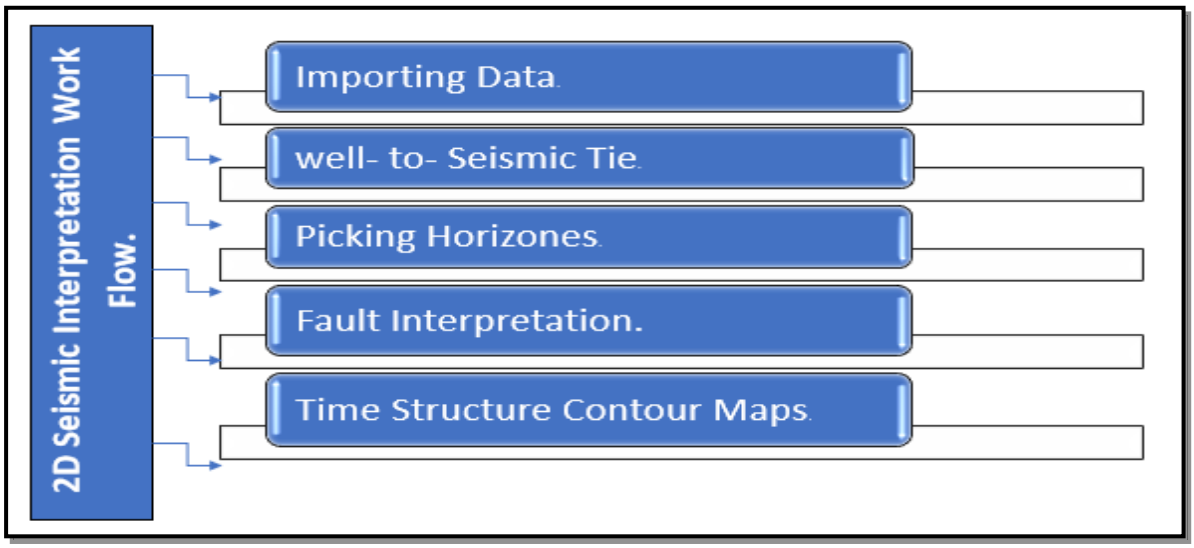

Fig. 6. Work flow of seismic interpretation

4.2.1 Well to seismic tie

The seismic tie (chronology) to well is one of the most useful tools for precisely detecting the responses of the drilled anomalies in the seismic interpretation and for quickly and simply understanding them since it establishes the relationship between seismic reflection and stratigraphy **(Bacon *et al.*, 2003; El Kadi *et al.*, 2020)**. To determine the acoustic impedance log, it is necessary to measure density log and the sonic log of the formation. Then, a time series of reflection coefficients was produced using the acoustic impedance and velocity data. This illustration (Fig. 7) reveals generally satisfactory results, regarding the connections between the generated synthetic

seismograms and the actual seismic data. The input seismic wavelet was chosen to match as closely as possible to produce during the original seismic acquisition, paying particular attention to the phase and frequency content, revealing the formation's top and bottom as well as zones of sand.

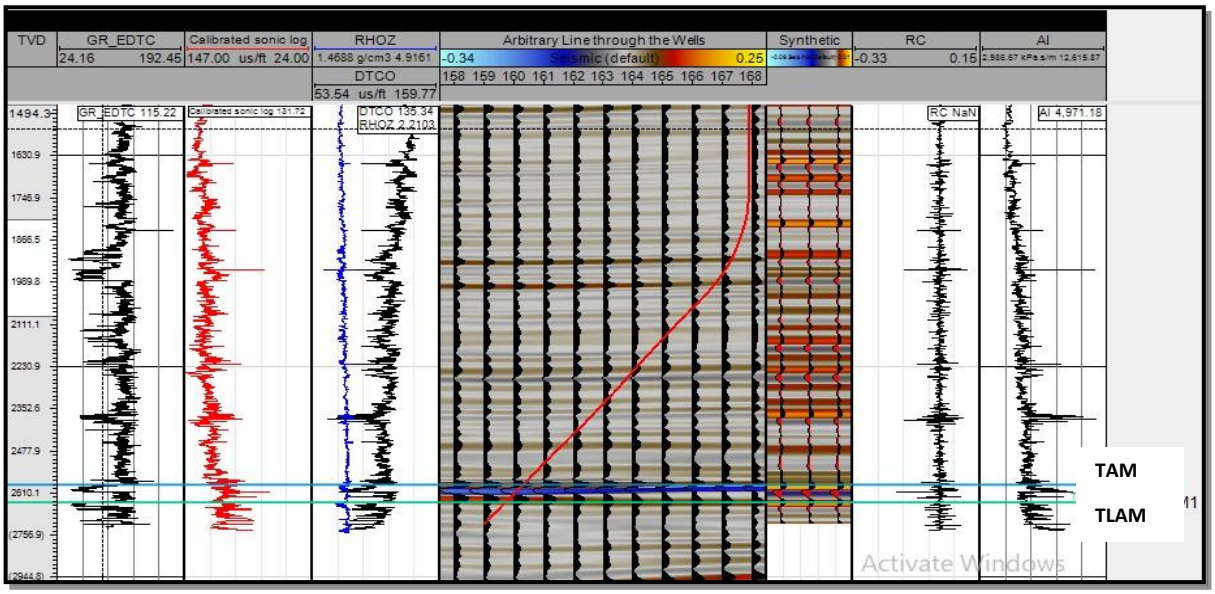

Fig. 7. Synthetic seismogram of SF-6 well

4.2.2 Piking of the horizons

In a following step, time data can be produced by selecting particular horizons on seismic lines, which aids in creating time structure contour maps of the selected horizons tops. These maps are useful for mapping desired outlines and calculating the quantities of specific accumulations of hydrocarbon reservoir. Four horizons were chosen for interpretation, based on the well-to-seismic tie process. The top Abu Madi Formation (shown in white color), top of Lower Abu Madi I zone (LAM I), top of zone lower Abu Madi II, and top of Qwasim Formation are the four horizons chosen for interpretation, as shown in Figs. (8- 10).

4.2.2.1 Top Qwasim Formation (Bottom of Abu Madi Formation) (white color)

Generally, this horizon has high seismic definition and continuity throughout the west El Manzal field (white color). The series of Abu Madi are angular with the underlying beds that are frequently quite apparent, and the Formation onlaps with the latter's truncated series. The explanation is based on the obviously large angular unconformity at the base of the Abu Madi Formation. Although there are cases when the horizon can be difficult to follow at a regional scale, as shown in Figs. (8- 10), the base's erosional geometry of the stratigraphic surface and the onlapping of above horizons give a good chance.

4.2.2.2 Top Lower Abu Madi Level II (black color)

The interpretation of this horizon (black line) is a locally continuous seismic peak whose amplitude is correlated with a decrease in seismic velocity. where gas-bearing sand displays a marked decrease in acoustic impedance, the strength of the reflection changes visibly and is stronger along the section (Fig. 10) in NE-SW direction.

4.2.2.3 Top Lower Abu Madi Level I (black color)

The seismic signal is well defined everywhere because of lateral changes in lithology and facies, which reflect a change from an overlaying series of more sand to more shaly Abu Madi layers. The interpreted horizon (black line) in the cross line 10 shown in (Fig. 10) follows seismic peaks with strong continuity throughout the whole study area. In general, the seismic features improved as one moved north and south, with the onshore seismic section covering the north and south part of the area at F-1, SF-2 wells.

4.2.2.4 Top of Abu Madi Formation (white color)

The interpreted surface (White line) follows a strong through-peak couplet that is continuous with a zero-crossing value that identifies a decrease in seismic velocity. It is created in the northern section as a result of the Kafr El Sheikh Formation's base having a "fast" sandstone level. The seismic definition over the entire area is quite good because of appearance to disappearance of these sands in southward of the survey, however, it seems to weaken progressively northward, where interpretation is very hard. This is because the acoustic impedance contrast at the contact between the Abu Madi Formation's late Messinian and Pliocene series cannot always accurately identify the horizon that appears clearly in sections over the studied area (Figs. 8 to 10). The lithology where the contact occurs is frequently very similar.

The Top Lower Abu Madi I and The Top Lower Abu Madi II stratigraphic levels were interpreted and correlated across all of the available wells; however, the quality and continuity of the interpreted seismic horizons (which are the major gas reservoirs in the Nile Delta region in general) remarkably vary from level to level and, for the same seismic horizon, from zone to zone, making it sometimes difficult to interpret sand facies areal distribution.

Finally, the Arbitrary seismic line, passing by all of studies wells in the area. The two gas fields of the research region are distributed along by Top and Lower's Abu Madi major display nearly smoothly, with thickness showing little differences between areas. According to analysis, the seismic lines are NE-SW orientated, and the chosen seismic sections in NW-SE direction as follows from: (Figs. 8 to 10) show how the form of a paleo valley gradually changed as it moved towards the north. demonstrating how the valley incision is shallower and less obvious in the southern most regions than on the northern part, where the valley profile seems larger and steeper.

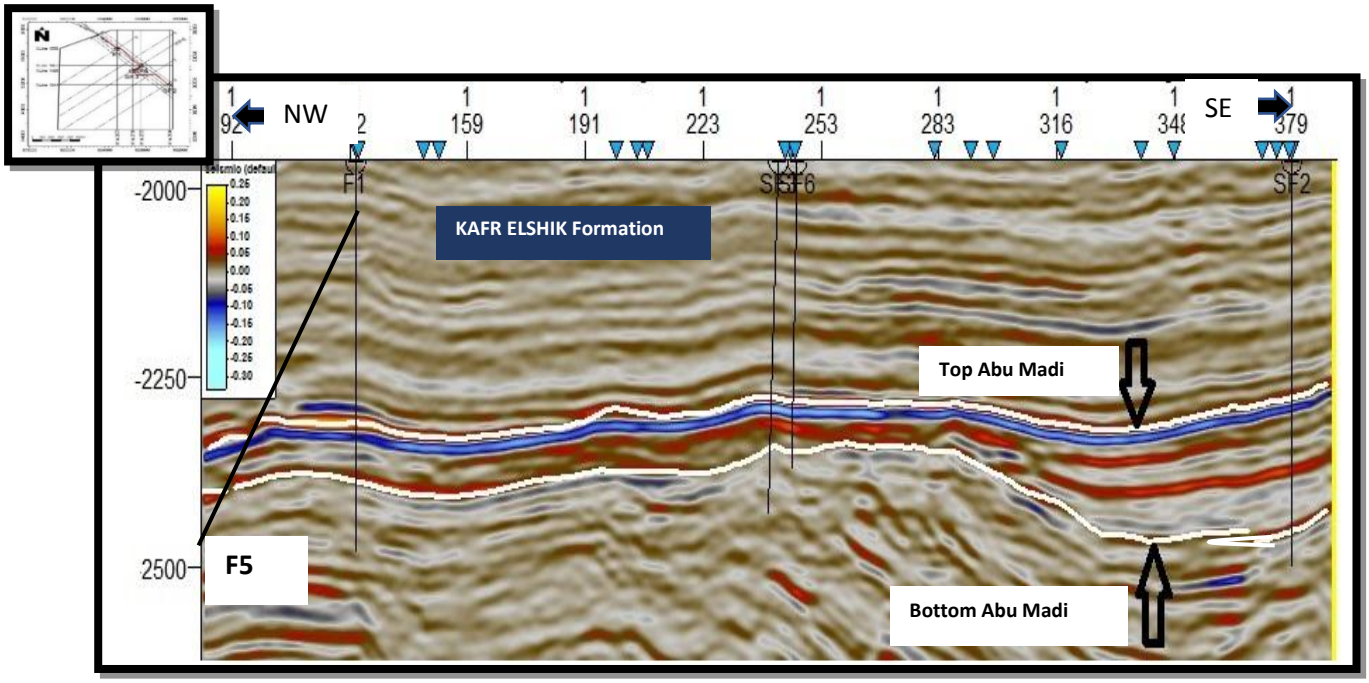

Fig. 8. Arbitrary Line Pass Through the Study Area and Wells With NW-SE Direction.

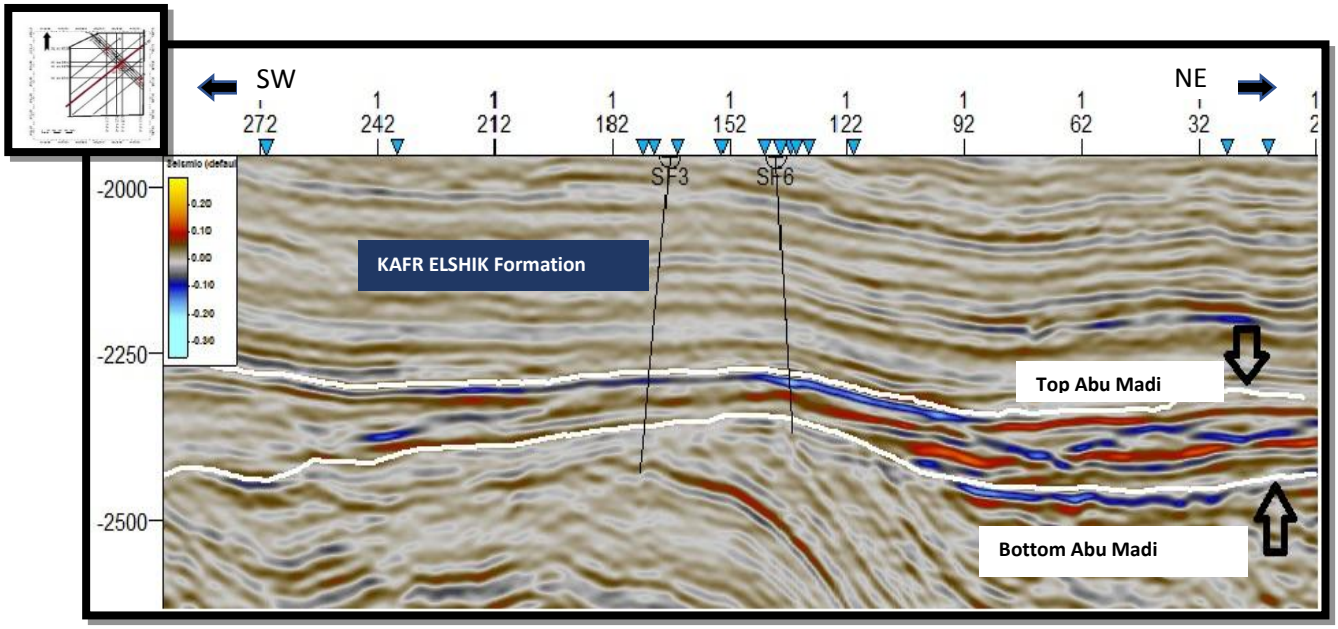

Fig. 9. Crossline 10 Pass Through the Study Area and Wells With NE-SW Direction**.**

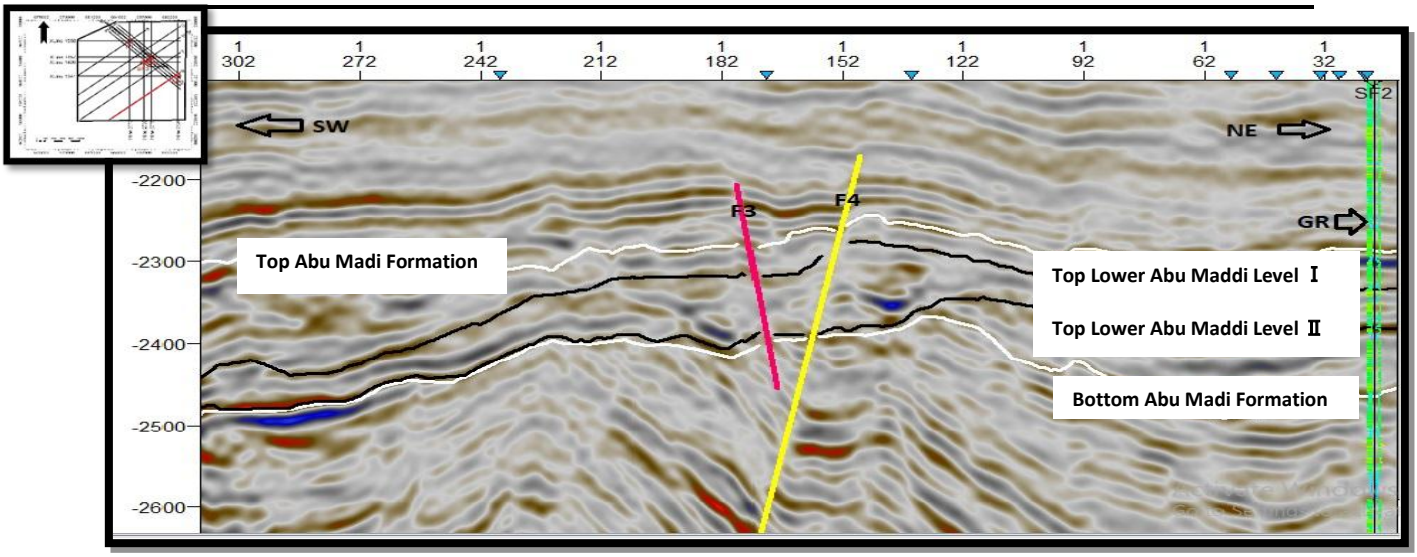

Fig. 10. Seismic Line 8 pass through SF-2 and Gama Ray Log (GR) of this Well With NE-SW Direction.

The two-way time of these horizons is mapped using the selected time of the Miocene reflectors along all seismic sections. In view of this, four isochronous (TWT) maps are displayed on Top of Abu Madi Formation, Top Abu Madi Level Ⅰ, Top Abu Madi Level Ⅱ and top Qwasim Formation (bottom of Abu Madi) as shown in (figs.11. A to D). The contoured maps show the formation top times in (ms), along with any possible faults that might cut across these tops. The following factors affect the maps' quality: 1) Data intensity, 2) Accuracy of seismic interpretation, and 3) Mapping parameters. The interpretation of the isochronous maps, which involves explaining the seismic data in terms of subsurface geologic information, comes after the development of the isochronous maps.

4.3.1 Time structure contour map on top of Abu Madi Formation

The top Abu Madi Formation isochronous map (Fig. 11A) shows a great variation in times, from the northeast to southwest direction. The higher anomaly (red) locates in the south eastern part; while the lower anomaly (blue) occupies the north western portion of the study area. The minimum value (shallow time) reaches -2180 ms to the south of SF-2well, while the maximum value (large time) attains -2520ms to the west of F-1 well, that mean time increase towards north west and in F-1 well, and decrease towards the south east in SF-2well.The time increase towards the north direction where the northern area controlled by two normal faults (F1 Fault), with the trend NNW-SSE and dipping to the west, (F5 Fault) the trend of this fault is NE- SW and its dipping to the north direction. The south part effected by two normal faults with same direction NW-SE and different dipping as (F4) with dipping to the south and (F3) with dipping to the north.The west side of the area affected by two normal faults (F6) and (F7) with the same direction

NE-SW, and different dipping as (F6) with dipping to the south west, and the dipping of (F7) fault is to the north west. All these faults extend in all mentioned tops.

4.3.2 Time structure contour map on top of Abu Madi Level Ⅰ

The time structure contour map on the top reveals Abu Madi Level Ⅰ (Fig11.B) varies between -2200, and -2400ms. Where, we can find the lowest time values of the surface map located in the south of SF-2 well. The highest value located North West of well F-1, where the northern area controlled by two normal faults (F1 Fault), with the trend NNW-SSE and dipping to the west as well as, (F5 Fault) the trend of this fault is NE- SW and its dipping to the north direction. The south part effected by two normal faults with same direction NW-SE and different dipping as (F4) with dipping to the south and(F3) with dipping to the north. Regionally, low relief features can be seen on the surface with time increasing toward the North.

4.3.3 Time structure contour map on top of Abu Madi Level Ⅱ

The time structure contour map on Top of Abu Madi Level II (Lower Abu Madi II) (Fig11.C), exhibits that, values of two-way time (TWT) of the surface map between -2240, and -2520ms. In addition, it shows an increasing in time values (TWT) toward the west and north west part of the map with value reaches -2520ms, while the lowest time value, which is at the map's center and has a time value of -2240ms. On common, the surface shows low relief feature with increasing in time to the north, while the map reveals also low steep degree of slope in the south area, that become more steeper to the north. Structurally, there are two normal faults affected in north and two other normal faults in the south part of the area these faults are the same faults which affected in the top of Abu Madi Level Ⅰ, there is a normal fault (F8) EES - WWN direction with dipping towards the north appears in the center of the map, also the other normal fault attains in south east with (F9) NNE-SSW direction and with dipping towards the south east.

4.3.4 Time structure contour map on the top of Qwasim Formation (Bottom of Abu Madi Formation)

The time structure contour map on top of Qwasim Formation (Fig 11.D); shows the surface TWT varies between -2260, and -2500 ms. The map reveals an increasing in time values toward the all parts of the map with value up to -2500 ms, but decrease in south east towards the center of the map in SF-3 and SF-6 wells. It is clear to the vision that the surface shows many relief features with increasing in time to the north, it is showing the valley passing through the area runs from south to north direction.

Finally, the area shows the erosional shape of the ancient paleo valley, that reflects sea transgression. The area is aff ected by eight high angle dip normal faults, with

different trends as follow: F1 Fault, with the trend NNW-SSE and dipping to the west,F5 Fault the trend of this fault is NE -SW and its dipping to the North,F4 and F6 Faults the trends of these Faults is WWN-EES with dipping to the South, F7 and F8 Faults with trend NE -SW and dipping to the North ,F9 Fault with trends NNE -SSW and its dip to the south east ,and F3 Fault with trend NW-SE and dipping to the north.

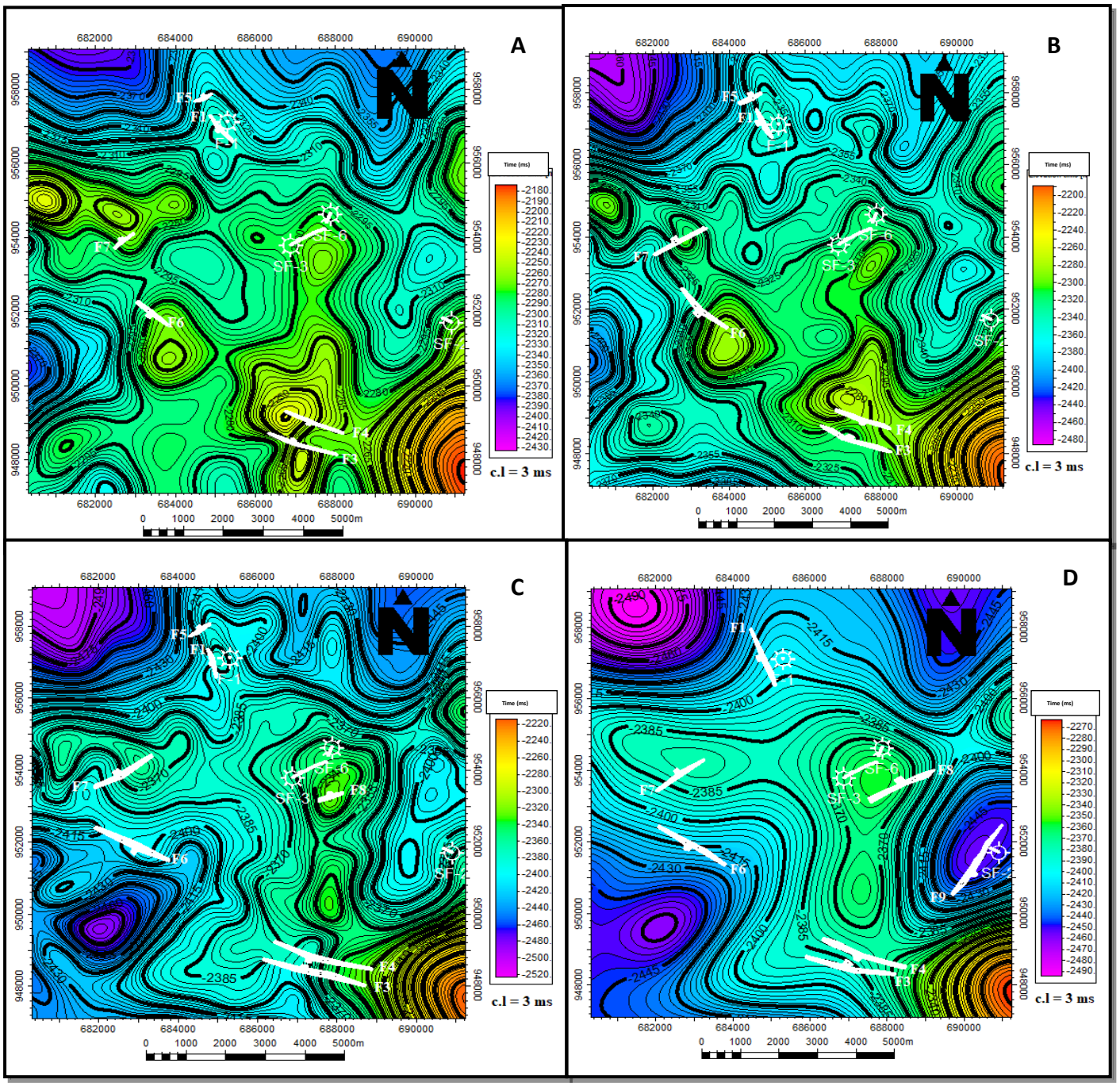

Fig.11. Time structure contour map on the top of Abu Madi Formation. (A) Top Abu Madi, (B) Top Abu Madi Level I, (C) Top Abu Madi Level I I, (D)Top Qwasim Formation.

Seismic attributes analysis can play a significant role in the reservoir's property prediction by revealing information that may not be evident in the standard amplitude data. A suite of properties of seismic trace (such as amplitude, phase, and frequency) can be cross plotted with the well logs to find the relation between the two types of data. The attributes selected on the basis of correlation with the petrophysical property can be effective in estimating reservoir properties away from the wells. Many seismic attributes have been used in reservoir characterization. A measurement based on seismic data is referred to as an attribute. Such as envelope amplitude (also known as "reflection strength"), instantaneous phase, instantaneous frequency, polarity, velocity, dip, dip azimuth, etc. **(Sheriff, 1994)**. Measurements of geometric, kinematic, or statistical properties emerging from seismic data are known as seismic attributes **(Chen and Sidney, 1997)**. It can be described as all seismic parameters **(Coren *et al*., 2001)**. The use of certain attributes to identify certain Miocene channels that reflect bright spots and flat spots (hydrocarbon indicators) and helps in the interpretation of seismic geomorphology (unconformities, lithology change, facies analysis, Faults, and channel features) as shown in the following steps:

4.4.1 Relative Acoustic Impedance (RAI)

This attribute calculates the trace's running sum after applying a low-cut filter. In a relative sense, it gave an indication of impedance changes. The approximate high frequency component of the relative acoustic impedance is represented by it. Using these attributes can help to show: Sequences boundaries, discontinuities, unconformity Surfaces, even the existence of fluid inside a hydrocarbon reserve, as well as porosity changes within the rocks. The result of application of Relative Acoustic Impedance (RAI) attributes (Fig.12.A) reveals different in impedance for many spots in the line reflecting major change in lithology through the study area. Zone 1 represents Abu Madi Formation by two spots of higher impedance in the EL Manzalla field in the channel, area between F1 well in the north, another spot located in the center of EL Manzalla Field, in SF3, SF6 wells. These areas containing hydrocarbon according to the petrophysics analysis. These two anomalies of high impedance are more visible by higher contrast between the positive and negative value of the section amplitude. Also, the presence of high fluid content inside the reservoirs led to contrast of relative acoustic impedance. The area between F1 well, SF6well and SF3 well show lower amplitude, reflects facies or even fluid types changes, dissimilar with these facies or fluids types located in the south in SF-2 well. Zone 2 marks the lower of the Pliocene (Kafr El-Sheikh Formation) with higher impedance in the north at SF-3, and SF-6 wells.

4.4.2 Signal Envelope (Reflection Strength)

The envelope is low frequency and only has positive amplitude, and it usually shows the major seismic features. The envelope is really important for identification

those features: Bright spots caused by gas accumulations and detection of gas accumulations, detection of major changes of lithology that are caused by strong energy reflection, sequence of boundaries, and unconformities. The result of application Reflection Strength (Signal Envelope) Attributes shown in Fig.12.B represent that This attribute method reflects strong response of amplitude for the anomaly of the Late Miocene sandstone of Top Abu Madi Formation and faint response for Bottom Abu Madi Formation and middle Kafr El-Sheikh Formation.

4.4.3 RMS Amplitudes And Reflection Intenisity

The square root of the sum of the squared amplitudes in a data set, divided by the sample size of data inside the specified time window, is known as the root-mean-square (RMS) amplitude, which is a computed seismic attribute. This attribute provides a statistical measure of the extent of variation in amplitude throughout a dataset, which is used to map hydrocarbon indications within a zone. RMS values will typically be larger where there are greater acoustic impedance changes (related to variations in stacked lithology). RMS amplitude that is greater in the extraction window is a good indicator of higher proportions of channel sands, or better reservoir facies, especially when coupled with higher attenuation levels. . The results of the application of mean root square (RMS) and reflection intensity attributes are shown in Fig.13.A-B.,these attributes methods reflect strong response of amplitude for the anomaly of the Late Miocene sandstone of Abu Madi Formation and low response for middle Kafr El-Sheikh Formation.

4.4.4 Instantaneous phase

Instantaneous phase value is expressed in degrees ($-\pi$, π). It helps to find both continuity and discontinuity in events. It illustrates bedding very good. Phase along the horizon shouldn't in, concept, change. Changes may take place if there is a picking issue, if the layer shifts laterally as a result of "sink-holes," or due to other phenomena. The most useful instantaneous phase are: improving the reflectors' continuity in order to display the lateral continuity, discontinuities, faults, pinch-outs, and seismic stratigraphic patterns like offlaps and onlaps. Fig.14, shows the result of instantaneous phase attribute which reveals the continuity and discontinuity in the study section showing good continuity of layers of Abu Madi Formation, gives the chance to easily tracking the horizon applying on arbitrary line Pass Through the study area and wells with NW-SE Direction.

4.4.5 Instantaneous Frequency And Dominant Frequency

It is the rate at which the phase changes, and it reflects the wavelet's mean amplitude or the phase's time derivative, gas reservoirs work to reduce the high frequencies more than rocks without gas saturation. This indicator has been determined to be rather unreliable by **Brown (2004);** several gas reservoirs examined with good data

have produced mysterious results in instantaneous frequency. The presence of this attributes can be utilized as a hydrocarbon indication, and method to detect the edges of low impedance thin beds, bed thickness, and chaotic reflection zone indicator.

Due to the oil presence in the pores, the unconsolidated sands sometimes focus to low frequency shadow. Lower frequency zones may represent a fracture zone, while higher frequencies reflect abrupt interfaces or thin shale bedding and lower frequencies sand-rich bedding. Fig(15-A) shows the dominant frequency attributes section, which reveals high frequency (green to blue color) dominate the whole section except the Top Abu Madi and Bottom Abu Madi Formation with lower frequency (yellow and yellowish green color) which reveals change in lithology or in fluids content. These two anomalies reflect lower frequencies zones (light blue and yellow to red color) as it shown in the instantaneous frequency attributes section in (Fig 15.B) which may be related to the existing of the sand reservoirs and the presence of hydrocarbon with different percentages in the Miocene section of the El Manzalla gas field.

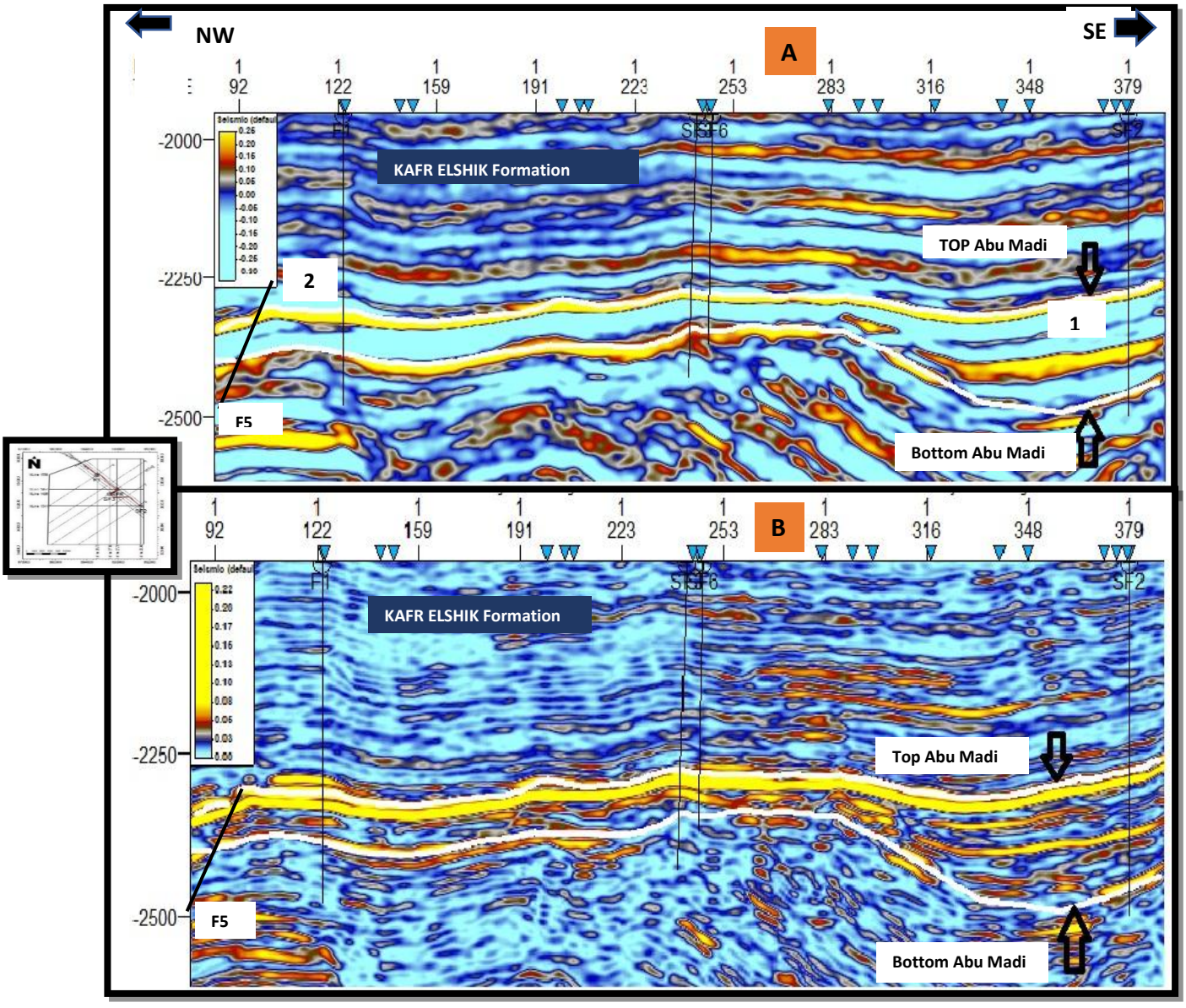

Fig. 12. (A) Relative Acoustic Impedance Attributes, (B) Reflection Strength (Signal Envelope) Attributes for Arbitrary Line Pass Through the Study Area and Wells With NW-SE Direction.

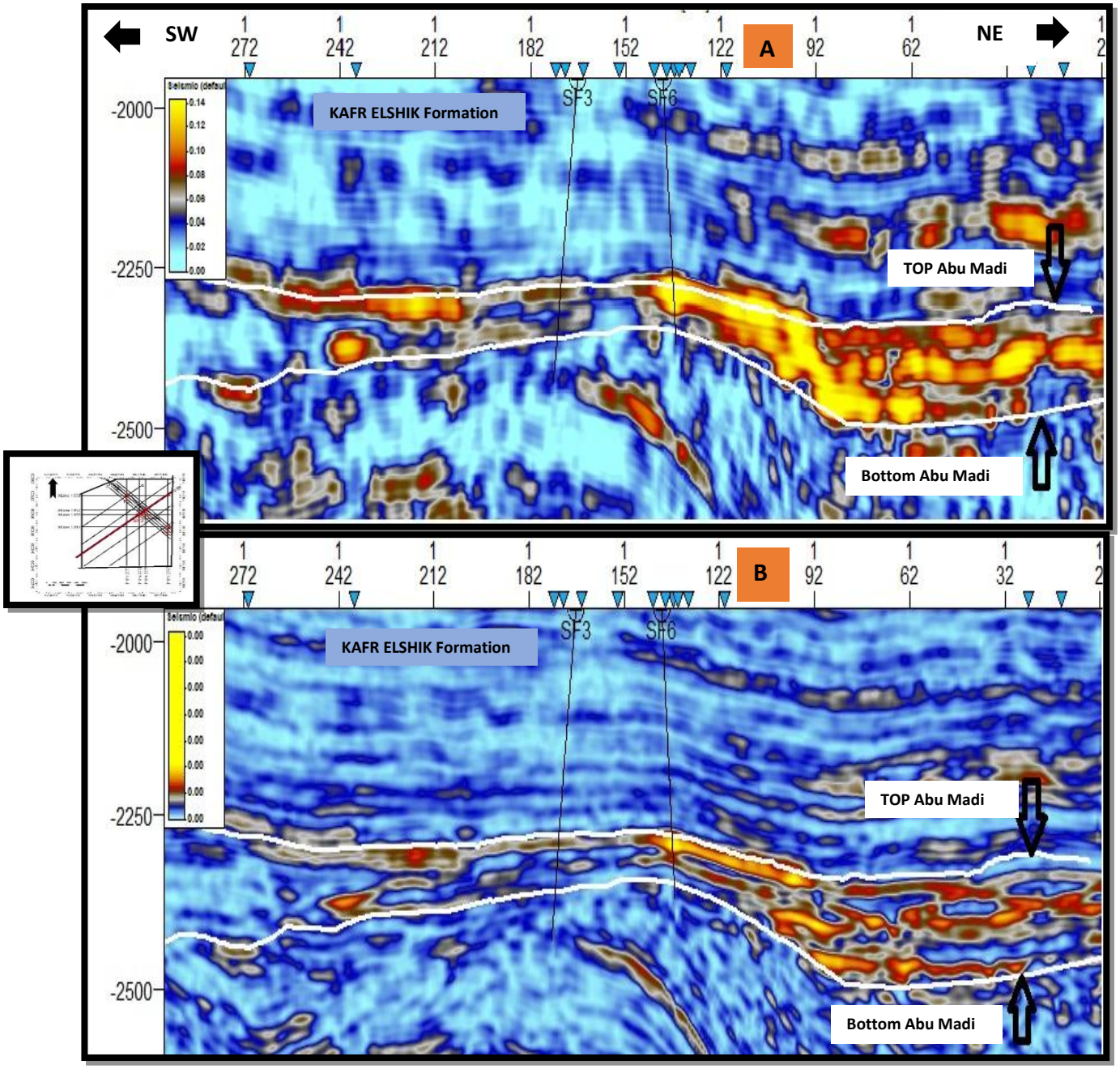

Fig. 13. (A) RMS Attributes, (B) Reflection Intensity Attributes for Crossline 10 Pass Through the Study Area and Wells With NE-SW Direction.

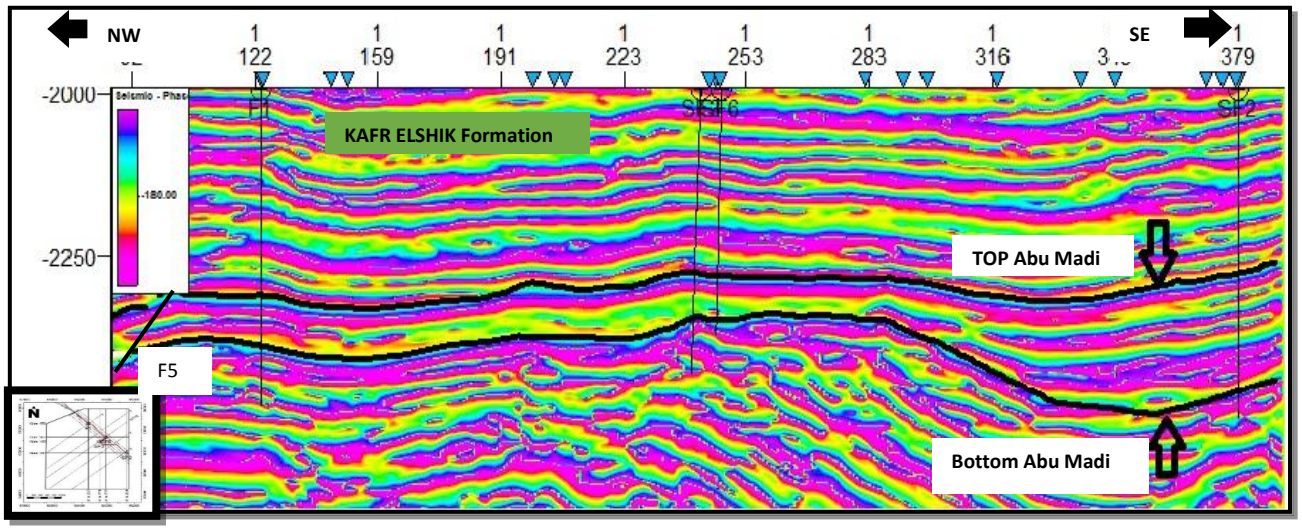

Fig (14) for Arbitrary line Pass Through the Study Area and Wells With NW-SE Direction After Applying Instantaneous Phase Attributes.

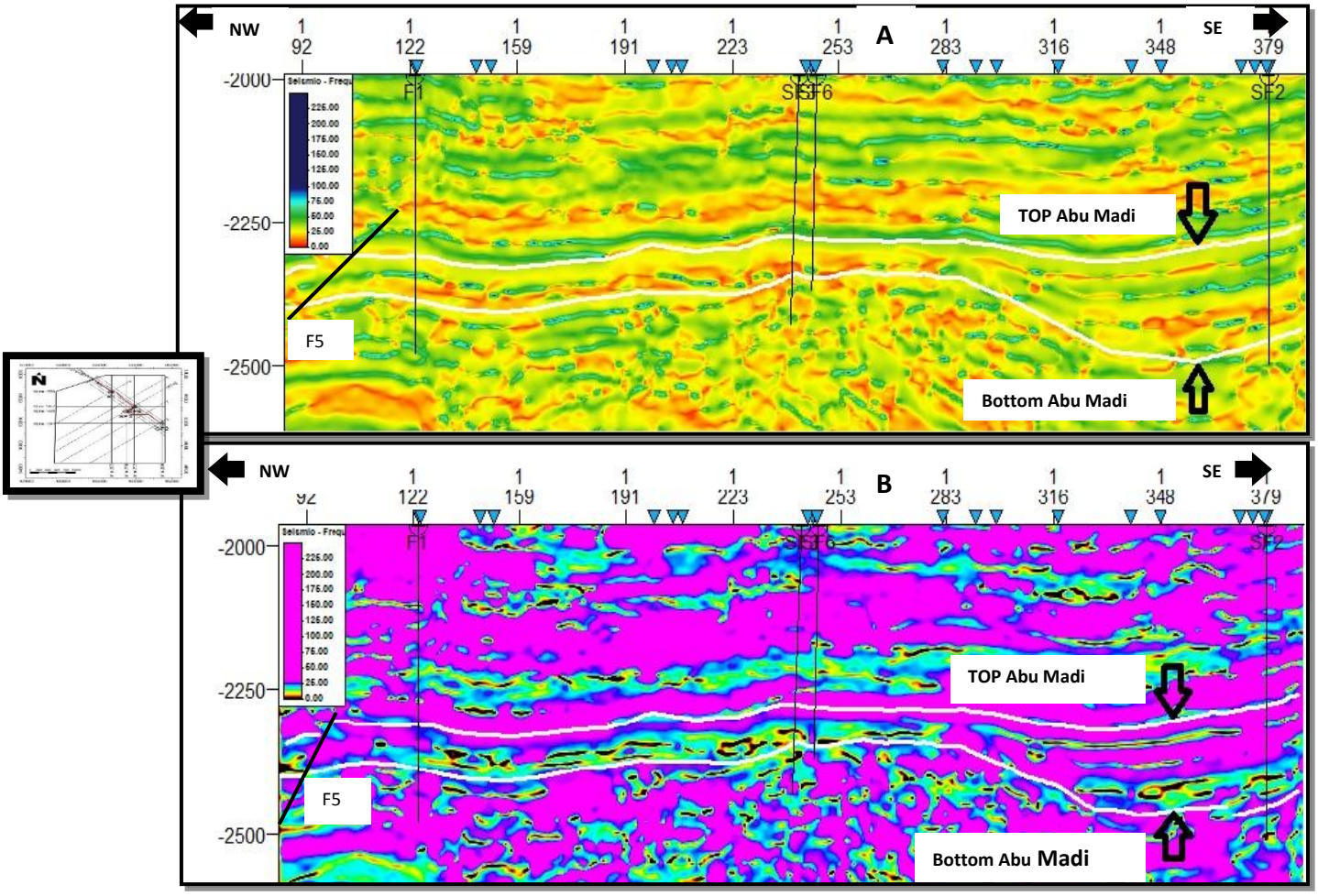

Fig. 15. (A) Instantaneous Frequency Attributes, (B) Dominant Frequency Attributes for Arbitary Line pass Through the Study Area and Wells With NW-SE Direction.

CONCLUSION

The arbitrary seismic line reveals an upper and lower section of the Abu Madi Formation. The upper Abu Madi is divided into two intervals: the first represents the main facies of the reservoir interval in the Upper Abu Madi in the West El Manzala field and it is composed of precisely fluvial channels of sandstone with shale and silt inter-bedded facies. It is distinguished by a non-reservoir part and is primarily composed of shale facies related to shallow marine and marks the abandon channel. And second interval which represent the main facies of reservoir interval in Upper Abu Madi in West El Manzala field and composed of exactly fluvial channels of sandstone with shale and silt inter-bedded facies. The reservoir quality is good inside the channel facies. The Lower Abu Madi is a pro deltaic sheet-like deposit that forms in an arbitrary line and has two facies characters: the first represents the upper zone, which is primarily non-reservoir shale with patches of anhydrite showing in some wells, and the second follows that and is primarily sandstone with inter beds of shale and siltstone.

A significant concentration of silty deltaic deposits and inter-fingering transgression marine shale give it its distinctive changeable reservoir quality. Seismic bright spots, which are typically located in the shallower part of the seismic section, are excellent indicators of gas or light hydrocarbon accumulations, particularly if a flat spot reflecting a possible gas-water contact is present. It can help the interpreter in getting more information from conventional seismic data, which can support the interpretation of geomorphology and paleo-environments. Major channels are the most common sorts of fluvial system components, and they are clearly displayed with envelope and RMS amplitude attribute. Through the application of some seismic attributes such as Signal Envelope (Reflection Strength), Instantaneous phase, Instantaneous Frequency, Relative Acoustic Impedance (RAI) and RMS Amplitudes, may be related to the existing of the sand reservoirs and the presence of hydrocarbon with different percentages in the Miocene section of the El Manzalla gas field.

ACKNOWLEDGEMENT

Authors acknowledge the Academy of Scientific Research and Technology (ASRT) for financial support provided through the SNG scholarship and the Egyptian Petroleum Research Institute (EPRI) for continuous support and help.

REFERENCES

Abdel Aal, A.; Price, R.; Vital, J. and Sharallow, J. (1994). Tectonic evolution of the Nile delta, its impact on sedimentation and hydrocarbon potential. In: Proceedings of 12th EGPC exploration and production conference, Cairo, Egypt, 1: 19–34.

Bacon, M.; Simm, R. and Redshow, T. (2003). 3-D Seismic interpretation, United Kingdom: Cambridge University Press.

Brown, A. R. (2004). Interpretation of three-dimensional seismic data (pp. 247-294, 6th ed.). American Association of Petroleum Geologists Memoir 42.

Chen and Sidney, S. (1997). Seismic attribute technology for reservoir forecasting and monitoring, The Leading Edge, pp.445-456.

Coren, F.; Volpi, V. and Tinivella, U. (2001). Gas hydrate physical properties imaging by multiattribute analysis-black ridge bsr case history, Marine Geology J., 178: 197-210.

Dolson, C.; Shaan. V.; Matbouly. S.; Harwood, C.; Rashed, R. and Hammouda, H. (2001) The petroleum potential of Egypt. In:Downey W, Threet C, Morgan A (eds) Petroleum provinces of the twenty-frst century. AAPG, 74: 453–482.

Dolson, J. C.; Boucher, P. J.; Siok, J. and Heppard, P. D. (2005). Key challenges torealizing full potential in an emerging giant gas province. Nile Delta/Mediterranean offshore, deep water, Egypt. Petrol Geol Conf series 6: 607–624.

EGPC (Egyptian General Petroleum Corporation) (1994). Nile Delta and North Sinai fields, discoveries and hydrocarbon potentials (A comprehensive overview). EGPC, Cairo, Egypt., 387 pp.

El Kadi, H. H.; Shebl, S.; Ghorab, M.; Azab, A. and Salama, M. (2020)."Evaluation of Abu Madi Formation in Baltim North & East gas fields, Egypt, using seismicinterpretation and well log analysis", NRIAG Journal of Astronomy and Geophysics.

El-Diasty, W.; Peters, K.; Moldowan, J.; Essa, G. and Hammad, M. (2020) Organic geochemistry of condensates and natural gases in the northwest Nile Delta ofshore Egypt. J Petrol Sci Eng 187:106819.

El-Gamal, M. and El-Bosraty, M. (2008). The Driving Forces behind the Tectonics and Evolution of the Southeastern Mediterranean, with the Hydrocarbon Systems Relationship and Future Discoveries. Mediterranean Offshore Conference. MOC 2008, Alex. Egypt, 69pp.

Leila, M. and Moscariello A. (2017). Organic geochemistry of oil and natural gas in the West Dikirnis and El-Tamad felds onshore Nile Delta, Egypt, Interpretation of potential source rocks. J Petrol Geol 40:37–58.

Leila, M. and Moscariello, A. (2019). Seismic stratigraphy and sedimentary facies analysis of the pre- and syn-Messinain salinity crisis sequences, onshore Nile Delta, Egypt, Implications for reservoir quality prediction. Mar. Petrol. Geol., 101: 303-321.

Leila, M.; Kora, M.; Ahmed, M. and Ghanem, A. (2016). Sedimentology and reservoir characterization of the upper Miocene Qawasim Formation, El-Tamad oil feld onshore Nile Delta, Egypt. Arab J Geosci 9:1–13.

Leila, M.; Moscariello, A.; Kora, M.; Mohamed, A. and Samankassou, E. (2020). Sedimentology and reservoir quality of a Messinian mixed siliciclastic carbonate succession, onshore Nile Delta, Egypt. Mar. Petrol. Geol., 112: 104076.

Mondal, S.; Chatterjee, R. and Chakraborty, S. (2021). An integrated approach for reservoir characterization in deep-water Krishna-Godavari basin, India: a case study.J. Geophys. Eng. 18 (1): 134-144.

Pigott, J. D. and Radivojevic, D. (2010). Seismic Stratigraphic Based Chronostratigraphy (SSBC) of the Serbian Banat Region of the Basin (Pannonian Basin). Cent Eur J Geosci 2(4):481–500.

Rizzini, A.; Vezzani, F. and Milad, G. (1978). Stratigraphy and sedimentation of a neogene quaternary section in the nile delta area. Mar. Geol. 27: 327-348.

Said, R. (1990). The Geology of Egypt. Balkema, Rotterdam.

Salem, A. M.; Ketzer, J. M.; Morad, S.; Rizk, R. R. and Al-Aasm, I. S. (2005). Diagenesis and reservoir-quality evolution of incised valley sandstones, evidence from the Abu Madi gas reservoirs (Upper Miocene), the Nile Delta Basin, Egypt. J Sed Res 75:572–584.

Sestini, G. (1989). Nile Delta: a review of depositional environments and geological history, in Whately, M. K. G., and Pickering, K. T., eds., Deltas: sites and traps for fossil fuels. Geological Society, London 41 (Special Publication): 99-127.

Sestini, G. (1995). Egypt. In: Kulke, H. (Ed.): Regional Petroleum Geology of The World, Part II: Africa, America, Australia and Antarctica (Beiträge zur regionalen Geologie der Erde 22: 66-87, Gebrüder Borntraeger Verlagsbuchhandlung, Stuttgart.

Shehata, A. (2008). Geological and petrophysical studies on Miocene oil reservoir of the deep target Sidi Salem sandstone, onshore Nile Delta, Egypt, MOC, Alex. Egypt, abstract.

Sheriff, R. E. (1994). Encyclopedia Dictionary of Exploration Geophysics, Soc. Expl. Geophys.

Vail, P. R.; Mitchum, RM. Jr. and Thompson, S. III. (1977). Seismic stratigraphy and global changes in sea level, part four, global cycles of relative changes of sea level. AAPG Mem 26:83–98.

Vandre, C.; Cramer, B.; Gerling, P. and Winsemann, J. (2007). Natural gas formation in the western Nile Delta (Eastern Mediterranean), thermogenic versus microbial mechanisms. Org Geochem 38:523–539.